Multi-Rays UWB Channel Modeling Based on Friis' Formula

Sathaporn Promwong[§†], Jun-ichi Takada[§], Navarat Lertsirisopon[§],
Pichaya Supanakoon[†] and Prakit Tangtisanon[†]

[§]Graduate School of Science and Engineering,
Tokyo Institute of Technology
2-12-1, O-okayama, Meguro-ku, Tokyo 152-8552, Japan.
Tel: +81 3 5734 3288, Fax: +81 3 5734 3282
E-mail: {ken,takada}@ap.ide.titech.ac.jp

[†]Department of Information Engineering, Faculty of Engineering,
King Mongkut's Institute of Technology Ladkrabang
Chalongkrung Road, Ladkrabang, Bangkok 10520, Thailand.
Phone: +66 2 7373000 ext. 5054, Fax: +66 2 3264176
E-mail: {kspichay,ktprakit}@kmitl.ac.th

Abstract

In this paper, UWB channel is modeled by using multi-ray technique. There are three case studies. The first case concerns only the normal direct path. The second one considers two rays that consist of the direct and ground reflection paths. And the last case considers the direct, ground and ceiling reflection paths. These cases are used to approximately model the UWB channel in the anechoic chamber, outdoor and indoor environment, respectively. The transmitted and received antennas use the trapezoidal antenna and perform the same characteristics. The impulse responses of these antennas at each specific pointing angles are calculated by using FDTD method and transformed to the far field region that are shown. The channels of these models are free space and apply in the Friis' transmission formula. The UWB channel impulse responses of each case are illustrated. After that, the transmitted signal is set to be a modulated Gaussian pulse within frequency ranges between 3.1 and 10.6 GHz. The matched filter reception is considered to maximize the SNR at the receiver for the evaluation. The received signal of each UWB model are shown. The effect of each UWB channel are described in the results.

Keywords: Ultra wideband (UWB), Friis' transmission formula, finite difference time domain method

1. Introduction

Recently, a new development in wireless communication known as Ultra-Wideband (UWB) radio is interested among the researchers. There are two main differences between UWB and other radio wave (RF) technology. Firstly, the bandwidth of UWB system defined by the Federal Communications Commission (FCC) [1] is more than 25 percents of a center frequency or more than 1.5 GHz, which is obviously much greater than the bandwidth used by any current communication technology. Secondly, the UWB is generally implemented by transmission of very short pulse without benefit of modulation onto a carrier frequency. Moreover, the power density of UWB signal is considered to be noise for the other communication systems because of its spectrums less than the noise level. Therefore, other receivers would not receive the UWB signal. The UWB receiver gathers the received signal power to regenerate the pulse. As a result, the UWB radio technology can exist with other RF technologies without interference.

Nevertheless, it is difficult to design the antenna for UWB system because in general narrow band systems, the conventional antennas are designed at only one frequency. If the impulse is excited to these antennas, the pulse will substantially distort and have the time dispersion. As a result, this leads to the increasing complexity of detection mechanism at the receiver [2]. Hence, the trapezoidal antenna is developed for the ultra wideband antenna [3].

The channel modeling is important part in order to predict the maximum allowable data rates in the intersymbol interference and the exploration of such techniques as diversity and equalization. There has been an appreciable amount of work to model the indoor propagation channel [4]-[7]. The transmission waveform and the matched filter reception are proposed in the extension of the Friis' transmission formula to UWB [8].

In this paper, UWB channel is modeled by using multi-ray technique. There are three case studies. The first case concerns only the normal direct path. The second one considers two rays that consist of the direct and ground reflection paths. And the last case considers the direct, ground and ceiling reflection paths. These cases are used to approximately model the UWB channel in the anechoic chamber, outdoor and indoor environments, respectively. The transmitted and received antennas use the trapezoidal antenna and perform the same characteristics [8]-[9].

CM02

The impulse responses of these antennas at each specific pointing angles are calculated by using FDTD method and transformed to the far field region that are shown. The channels of these models are free space and apply in the Friis' transmission formula. For this simulation structure, Both transmitted and received antenna heights are set to be 2 m far from the floor and separated by 1 m. For the third case, the ceiling height is set to be 5 m far from the floor. The reflection coefficients of the ground and ceiling are also considered. The UWB channel impulse responses of each case are illustrated. After that, the transmitted signal is set to be a modulated Gaussian pulse within frequency ranges between 3.1 and 10.6 GHz. The matched filter reception is considered to maximize the SNR at the receiver for the evaluation. The received signal of each UWB model are shown. The effects of each UWB channel are described in the results.

2. FDTD Method

The finite difference equations are derived directly from Maxwell's curl equations in the time-domain. To obtain discrete approximation of the continuous partial differential equations, the centered difference approximation is used on both the time and space first-order partial differences. The entire computation domain is the collection of all the unit cells. After simple arrangement, the finite difference equations are described in [10]. The maximum time step is limited by the stability restriction of finite difference equation [11].

A voltage source V_S is represented as an electric field E in the y direction at the node i_S, j_S and k_S along x, y and z axis, respectively. If the source resistance is set to R_S, then the usual FDTD electric field at the source location is given by [12]. This resistive voltage source model is used to consider the antenna as the one-port network and excite the voltage signal to the antenna.

The tangential field components on the six mesh walls must be specified in such a way that outgoing waves are not reflected. In this paper, the perfectly matched layer absorbing boundary condition (PML ABC) [13] is used. The PML ABC can absorb propagation wave effectively by using nonphysical lossy media adjacent to the outer-grid boundaries backed by perfectly conducting walls.

For the electromagnetic analysis by using FDTD method, the provided data are near fields. Therefore, these near fields are transformed to far fields [14]-[15]. Then, the far fields are used to calculate the radiation pattern, far field transfer function and impulse response.

3. Extension of Friis' Transmission formula

For the UWB channel modeling, the channel is free space. The extension of Friss's transmission formula [13] is used. For the narrowband systems, Friss' transmission formula have been widely used

$$G_{Friis} = \frac{P_r}{P_t} = G_f G_r G_t, \tag{1}$$

where G_r and G_t are received and transmitted antenna gain, respectively,

$$G_f = \left(\frac{\lambda}{4\pi d}\right)^2 = \left(\frac{c}{4\pi df}\right)^2, \tag{2}$$

is the free space propagation gain (less than unity in practice), $\lambda = c/f$ is the wavelength, c is the velocity of the light, and f is the frequency.

Friis' formula is extended taking into account the transmission waveform as

$$\begin{aligned} H_{e-Friis}(\theta,\phi,f,d) &= \frac{V_r(f)}{V_t(f)}, \\ &= H_f(f)\mathbf{H}_r(\theta,\phi,f,d)\cdot\mathbf{H}_t(\theta,\phi,f,d), \end{aligned} \tag{3}$$

where $\mathbf{H}_a(\theta,\phi,f,d)$ is a complex transfer function vector of the antenna relative to the isotropic antenna, index a is r or t, V_t and V_r are the transmitted and received voltage signals, respectively.

The free space transfer function can be written as

$$H_f(\theta,\phi,f,d) = \frac{c}{4\pi d(\theta,\phi)f} e^{-j2\pi d(\theta,\phi)f/c}. \tag{4}$$

Unit vector $\hat{\theta}$ and $\hat{\phi}$ express the polarization which are defined respect to the local polar coordinates of the each of the antennas.

The impulse response of Friis's formula transmission $h_{e-Friis}(\theta,\phi,t,d)$ and matched filter $h_{MF}(\theta,\phi,t,d)$ can calculate by using inverse Fourier transform

$$h_{e-Friis}(\theta,\phi,t,d) = \mathscr{F}^{-1}\{H_{e-Friis}(\theta,\phi,f,d)\}, \tag{5}$$
$$h_{MF}(\theta,\phi,t,d) = \mathscr{F}^{-1}\{H_{MF}(\theta,\phi,f,d)\}, \tag{6}$$

where $\mathscr{F}^{-1}\{\cdot\}$ is inverse Fourier operator.

4. Multi-Rays UWB Channel Modeling

For the multi-rays UWB channel modeling used in this paper, the three case are studied. The first case considers one ray, the normal direct path. The second case considers two rays, the direct and ground reflection paths. And the final case considers the direct, ground and ceiling reflection paths. These cases are used to approximately model the UWB channel in the anechoic chamber, outdoor and indoor environments, respectively.

The received signal from the multi-rays UWB channel model is given by

$$v_r(t) = v_t(t) * h_{UWB}(t) * h_{MF-UWB}(t), \tag{7}$$

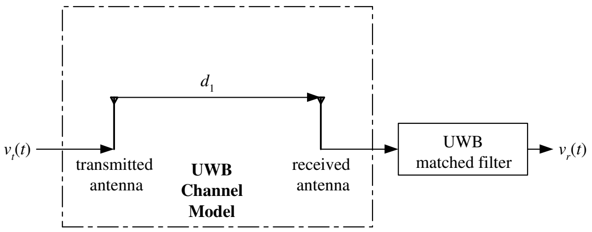

Fig. 1. One-ray UWB channel model.

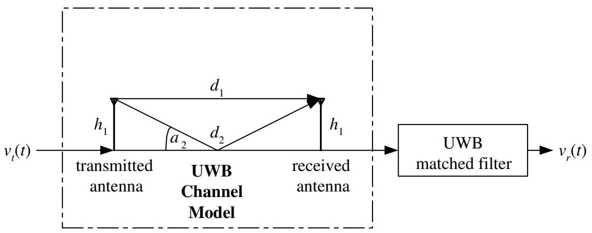

Fig. 2. Two-rays UWB channel model.

where $h_{UWB}(t)$ and h_{MF-UWB} are the UWB channel and matched filter impulse responses, respectively. $v_r(t)$ and $v_t(t)$ are the transmitted and received signals, respectively.

At the receiver, the UWB matched filter frequency transfer function $H_{MF-UWB}(f)$ is introduced to maximize the signal-to-noise ratio (SNR) of the receiver output,

$$H_{MF-UWB}(f) = \frac{H^*_{UWB}(f)}{\sqrt{\int_{-\infty}^{\infty} |H_{UWB}(f)|^2 df}}. \quad (8)$$

Therefore, the UWB matched filter impulse response is given by

$$h_{MF-UWB}(t) = \mathscr{F}^{-1}\{H_{MF-UWB}(f)\}. \quad (9)$$

4.1 One ray modeling

The one ray UWB channel modeling considers only direct path as shown in figure 1.

The UWB channel frequency transfer function and impulse response can be written as

$$H_{UWB}(t) = H_{e-Friis}(90^\circ, 0, t, d_1), \quad (10)$$
$$h_{UWB}(t) = h_{e-Friis}(90^\circ, 0, t, d_1), \quad (11)$$

where d_1 is the distance of the direct path.

4.2 Two rays modeling

The two rays UWB channel modeling considers the direct and ground reflection paths. Figure 2 shows the two ray UWB channel model.

The UWB channel frequency transfer function and impulse response can be written as

$$\begin{aligned} H_{UWB}(t) &= H_{e-Friis}(90^\circ, 0, t, d_1) \quad (12) \\ &\quad +\Gamma_2 H_{e-Friis}(\theta_2, 0, t, d_2), \\ h_{UWB}(t) &= h_{e-Friis}(90^\circ, 0, t, d_1) \quad (13) \\ &\quad +\Gamma_2 h_{e-Friis}(\theta_2, 0, t, d_2), \end{aligned}$$

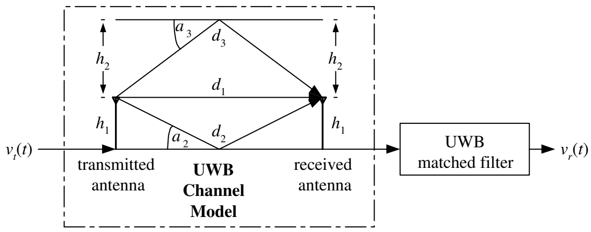

Fig. 3. Three-rays UWB channel model.

where d_2 is the distance of the ground reflection path which is defined by,

$$d_2 = \sqrt{4h_1^2 + d_1^2}, \quad (14)$$

h_1 is the transmitted and received antenna heights far from the floor and θ_2 is defined by

$$\theta_2 = 90^\circ + \tan^{-1}\left(\frac{2h_1}{d_1}\right). \quad (15)$$

Γ_2 is the plane wave Fresnel reflection coefficient. This model considers to be vertical polarized transmission and the floor do not have ferromagnetic characteristic. Then, the plane wave Fresnel reflection coefficient can be written as [16]

$$\Gamma_2 = \frac{\sqrt{\frac{1}{\varepsilon_2}} \cdot \sqrt{1 - \frac{1}{\varepsilon_2}\cos^2\theta_2} - \sin\theta_2}{\sqrt{\frac{1}{\varepsilon_2}} \cdot \sqrt{1 - \frac{1}{\varepsilon_2}\cos^2\theta_2} + \sin\theta_2}, \quad (16)$$

where ε_2 is the permittivity of the floor.

4.3 Three rays modeling

The three rays UWB channel modeling considers the direct, ground and ceiling reflection paths as shown in figure 3.

The UWB channel frequency transfer function and impulse response can be written as

$$\begin{aligned} H_{UWB}(t) &= H_{e-Friis}(90^\circ, 0, t, d_1) \quad (17) \\ &\quad +\Gamma_2 H_{e-Friis}(\theta_2, 0, t, d_2) \\ &\quad +\Gamma_3 H_{e-Friis}(\theta_3, 0, t, d_3), \\ h_{UWB}(t) &= h_{e-Friis}(90^\circ, 0, t, d_1) \quad (18) \\ &\quad +\Gamma_2 h_{e-Friis}(\theta_2, 0, t, d_2) \\ &\quad +\Gamma_3 h_{e-Friis}(\theta_3, 0, t, d_3), \end{aligned}$$

where d_3 is the distance of the ceiling reflection path which is defined by,

$$d_3 = \sqrt{4h_2^2 + d_1^2}, \quad (19)$$

h_2 is the transmitted and received antenna heights far from the ceiling and θ_3 is defined by

$$\theta_3 = 90^\circ - \tan^{-1}\left(\frac{2h_2}{d_1}\right). \quad (20)$$

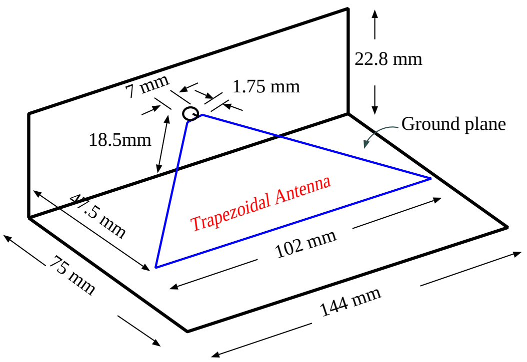

Fig. 4. Structure and dimensions of trapezoidal antenna.

Γ_3 is the plane wave Fresnel reflection coefficient. This model considers to be vertical polarized transmission and the floor do not have ferromagnetic characteristic. Then, the plane wave Fresnel reflection coefficient can be written as [16]

$$\Gamma_3 = \frac{\sqrt{\frac{1}{\varepsilon_3}} \cdot \sqrt{1 - \frac{1}{\varepsilon_3}\cos^2\theta_3} - \sin\theta_3}{\sqrt{\frac{1}{\varepsilon_3}} \cdot \sqrt{1 - \frac{1}{\varepsilon_3}\cos^2\theta_3} + \sin\theta_3}, \tag{21}$$

where ε_3 is the permittivity of the ceiling.

5. Numerical Results

UWB channel is modeled by using multi-ray technique. Three cases, which are one-ray, two rays and three rays, are studied. Both transmitted and received antenna heights are set to be $h_1 = 2$ m far from the ground and separated by $d_1 = 1$ m. For the third case, the ceiling height is set to be 5 m far from the ground. Then, the ceiling height is $h_2 = 3$ m far from both antennas. The distances of the ground and ceiling reflection paths are $d_2 = 4.12$ m and $d_3 = 6.08$ m, respectively. The angles of the ground and ceiling reflection paths are $\theta_2 = 165.96°$ and $\theta_3 = 9.46°$, respectively. The permittivity of the ground and ceiling are set to be 7 and 5, respectively. Therefore, the plane wave Fresnel reflection coefficient at ground and ceiling are $\Gamma_2 = 0.36$ and $\Gamma_3 = 0.49$, respectively

The trapezoidal antennas [3] are used in these models for the transmitted and received antennas. The structure and dimensions of the trapezoidal antenna is shown in figure 4. The far field impulse response and frequency transfer function of this antenna is computed by using FDTD method and transformed to the far field. The far field impulse responses at $(\theta = 0, \phi = 0)$, $(\theta = 165.96°, \phi = 0)$ and $(\theta = 9.46°, \phi = 0)$ are shown in figure 5. The magnitudes of the far field frequency transfer functions of the antennas at $(\theta = 0, \phi = 0)$, $(\theta = 165.96°, \phi = 0)$ and $(\theta = 9.46°, \phi = 0)$ are shown in figure 6.

The impulse responses of the one-ray, two-rays and three-rays UWB channel models are shown in figure

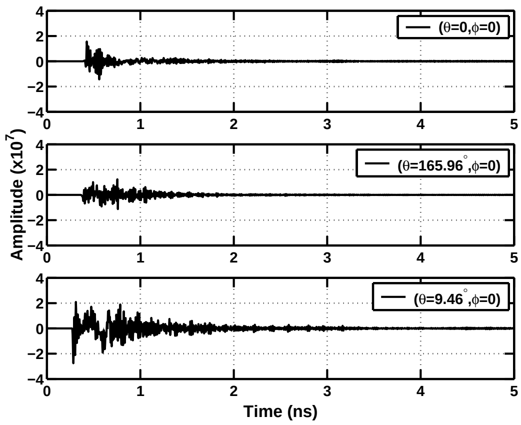

Fig. 5. Far field impulse responses of the transmitted and received antennas.

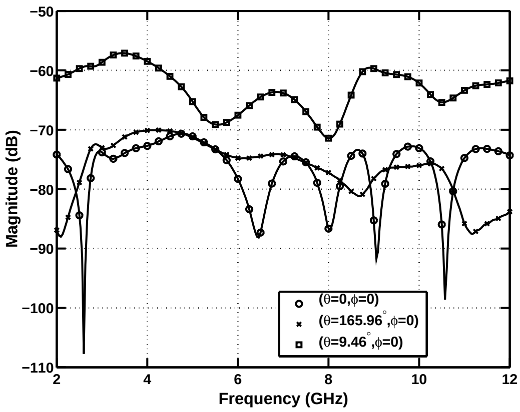

Fig. 6. Magnitudes of far field frequency transfer functions of the transmitted and received antennas.

7. Figure 8 shows the magnitudes of the frequency transfer functions of the one-ray, two-rays and three-rays UWB channel models, respectively.

The effect of the waveform distortion is observed. The modulated Gaussian pulse signal with spectrum ranges from 3.1 to 10.6 GHz is considered and its equation is

$$v_t(t) = e^{-[(t-3A)/A]^2} \sin(2\pi f_c t), \tag{22}$$

where f_c is 6.85 GHz and $A = 1.0949$. The waveform of this modulated Gaussian pulse signal is shown in figure 9.

The signal from the one-ray, two-rays and three rays UWB channel model are shown in figure 10. Figure 11 shows the received signal form the output of the matched filter.

6. Conclusions

In this paper, UWB channel is modeled by using multi-ray technique. Three cases are studied. The first case considers the normal direct path. The second case considers two rays, the direct and ground

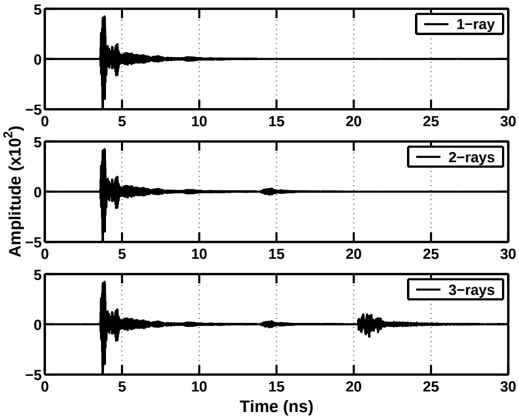

Fig. 7. Impulse responses of the one-ray, two-rays and three-rays UWB channel models.

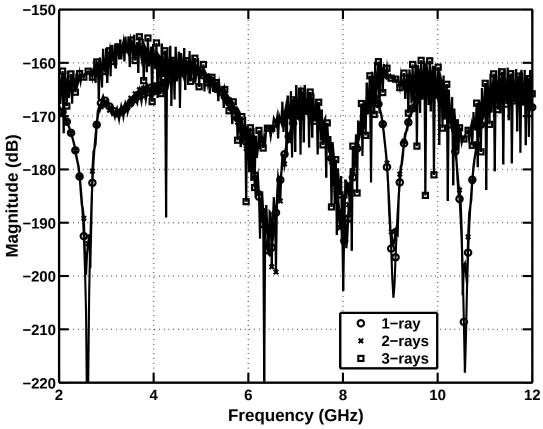

Fig. 8. Magnitudes of the frequency transfer functions of the one-ray, two-rays and three-rays UWB channel models.

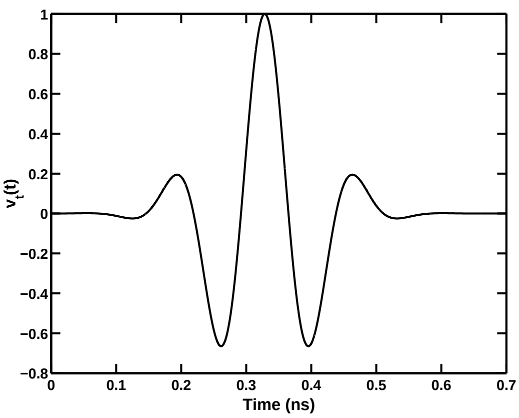

Fig. 9. Waveform of the modulated Gaussian pulse signal.

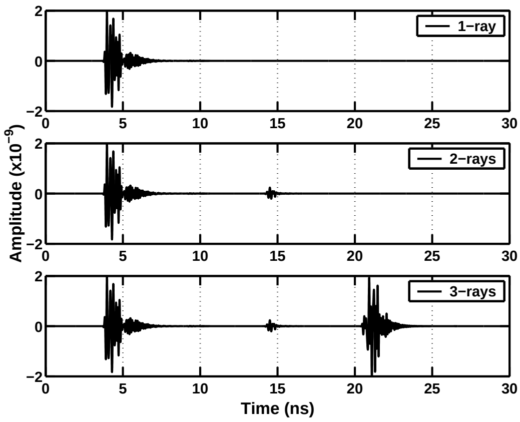

Fig. 10. Signal from the one-ray, two-rays and three rays UWB channel model.

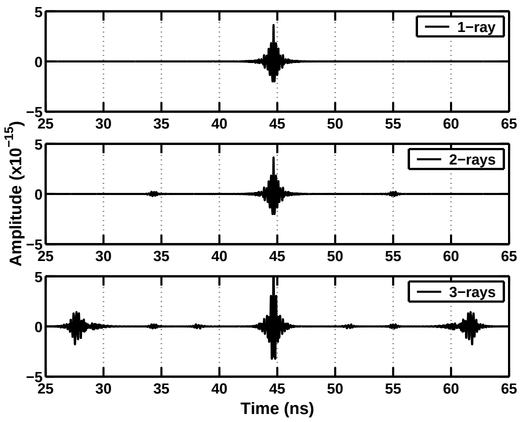

Fig. 11. Received signal from the output of the matched filter.

reflection paths. And the final case considers the direct, ground and ceiling reflection paths. From these results, we can see the effect of the signal distortion from each model. This multi-rays UWB channel modeling can be applied to use for the ray-splitting or ray tracing technique.

References

[1] Federal Communications Commission, "Revision of part 15 of the commission's rules regarding UWB transmission systems," First Report, FCC 02-48, Apr. 2002.

[2] K. Siwiak, "Impact of ultra wide band transmission on a generic reciever," *Proc. IEEE Veh. Tech. Conf. (VTC)*, vol. 2, pp. 1181-1183, May 2001.

[3] A. Duzdar and G. Kompa, "A novel trapesoidal antenna fed by a ground image plane and backed by a reflector," *Proc. Euro. Microwave Workshop (EuMC) 2000*, vol. 2, pp. 1-4, Paris, France, Sept. 2000.

[4] H. F. Harmuth and S. Ding-Rong, "Antennas for nonsinusiodal wave - part II: sensors," *IEEE*

Trans. Elec. Mag. Compat., vol. EMC-25, no. 2, pp. 107-115, May. 1983.

[5] H. Hashemi, "The indoor radio propagation channel," *Proc. IEEE*, vol. 81, no. 7, pp. 943-968, July 1993.

[6] H. Hashemi, "Impulse response modeling of indoor propagation channels," *IEEE J. Select. Areas Commun.*, vol. 11, no. 7, pp. 967-978, Sept. 1993.

[7] T. S. Rappaport, "Characterization of UHF multipath radio channels in factory buildings," *IEEE Trans. Antennas Propagat.*, vol. 37, no. 8, pp. 1058-1069, Aug. 1989.

[8] J. Takada, S. Promwong and W. Hachitani, "Extension of Friis' transmission formula for ultra wideband systems," *IEICE Tech. Rep., WBS2003-*/MW2003-**, May 2003.

[9] S. Promwong, W. Hachitani, and J. Takada, "Experimental evaluation scheme of UWB antenna performance," *IEEJ. IM2003-**, June 2003.

[10] K. S. Yee, "Numerical solution of initial boundary value problems involving Maxwell's equations in isotropic media," *IEEE Trans. Antennas Propagat.*, vol. AP-14, pp. 302-307, 1966.

[11] A. Taflove and M. E. Brodwin, "Numerical solution of steady-state electromagnetic scattering problems using the time-dependent Maxwell's equation," *IEEE Trans. Microwave Theory Tech.*, vol. 23, pp. 623-630, 1975.

[12] R. J. Luebbers and H. S. Langdon, "A simple feed model reduces time steps needed for FDTD antenna and microstip calculations," *IEEE Trans. Antennas Propagat.*, vol. 44, no. 7, pp. 1000-1005, 1996.

[13] J. P. Berenger, "A perfectly matched layer for the absorption of electromagnetic waves," *J. Computational Physics*, vol. 114, pp. 185-200, 1994.

[14] S. Ramo, J. Whinnery and T. Van Duzer, "Fields and Waves in Communication Electronics," 2nd ed., John Wiley & Sons, New York, 1984.

[15] R. J. Luebbers, K. S. Kunz, M. Schneider and F. Hunsberger, "A finite-difference time-domain near zone to far zone transformation," *IEEE Trans. Antennas Propagat.*, vol. 39, pp. 429-433, 1991.

[16] C. A. Balanis, "Advanced Engineering Electromagnetics," John Wiley & Sons, Inc. 1989.

Sathaporn Promwong received the B.E. degree in Electronics Engineering and M.E. degree in Electrical Engineering from King Mongkut's Institute of Technology Ladkrabang, Bangkok, Thailand, in 1994 and 1999, respectively. He is currently working toward the Ph.D. degree in Tokyo Institute of Technology, Tokyo, Japan.

Since 1995, he has joined in the department of Information Engineering, Faculty of Engineering, King Mongkut's Institute of Technology Ladkrabang. His research is interested in the area of Ultra Wideband (UWB) communications and antenna propagation. He is presently a member of the IEICE and IEEE.

Jun-ichi Takada was born in Tokyo, Japan in 1964. He received the B.E., M.E. and D.E. degrees from Tokyo Institute of Technology, Japan, in 1987, 1989 and 1992, respectively. From 1992 to 1994, he has been a Research Associate at Chiba University, Chiba, Japan. From 1994, he has been an Associate Professor at Tokyo Institute of Technology, Tokyo, Japan. His current interested are mobile propagation and channel modeling, array signal processing and numerical simulation of waves.

Dr. Takada received the Excellent Paper Award and Young Engineer Award from IEICE, Japan in 1993 and 1994, respectively. He is a member of the IEICE, ACES, SIAM and AGU.

Navarat Lertsirisopon graduated with a B.E. degree in Electrical Engineering from Sirindhorn International Institute of Technology, Thammasat University, Bangkok, Thailand in 2002. Her senior project involved the design of a data communication network using Genetic Algorithm (GA) and Memetic Algorithm (MA).

Presently, she is a research student in Tokyo Institute of Technology, Tokyo, Japan. Her current interest is in the area of Ultra Wideband (UWB) Technology.

Pichaya Supanakoon received the B.E. degree in Telecommunication Engineering and M.E. degree in Electrical Engineering both from King Mongkut's Institute of Technology Ladkrabang, Bangkok, Thailand, in 1998 and 2000, respectively.

Since 1999, he has been with the Department of Information Engineering, Faculty of Engineering, King Mongkut's Institute of Technology Ladkrabang, as Lecturer. His research interests are in electromagnetic field computation, finite-difference time-domain (FDTD) method, electromagnetic compatibility, and radio wave propagation.

Prakit Tangtisanon, photograph and biography not available at time of publication.